

MOL #109900

TITLE PAGE

**Identification of an Oleanane-type Triterpene Hedragonic Acid as a Novel Farnesoid X
Receptor Ligand with Liver Protective Effects and Anti-inflammatory Activity**

Yi Lu, Weili Zheng, Shengchen Lin, Fusheng Guo, Yanlin Zhu, Yijuan Wei, Xi Liu, Shikai Jin,
Lihua Jin and Yong Li

State Key Laboratory of Cellular Stress Biology, School of Life Sciences, Innovation Center for
Cell Signaling Network, Xiamen University, Xiamen, Fujian 361005, China

MOL #109900

RUNNING TITLE PAGE

Running title: Hedragonic acid as an FXR agonist

***Correspondence:** Dr. Lihua Jin, Rm D406 Huang Chao Yang building, Xiamen University, South Xiang An Road, Xiang An District, Xiamen, Fujian 361102, China, Tel: +86-592-2181560, Email: jinh@xmu.edu.cn; Dr. Yong Li, Rm D408 Huang Chao Yang building, Xiamen University, South Xiang An Road, Xiang An District, Xiamen, Fujian 361102, China, Tel: +86-592-2181510, Email: yongli@xmu.edu.cn.

Number of text pages: 29

Number of tables: 0

Number of figures: 6

Number of references: 43

Number of words in the Abstract: 221,

Introduction: 548,

Discussion: 472

Abbreviations: AlphaScreen, Amplified Luminescent Proximity Homogeneous Assay; ALT, alanine aminotransferase; APAP, acetyl-para-aminophenol; AR, androgen receptor; AST, aspartate aminotransferase; BA, bile acid; FXR, Farnesoid X receptor; GPBAR1, G-protein-coupled bile acid receptor 1; CA, cholic acid; CD, Circular Dichroism Spectroscopy; CDCA, chenodeoxycholic acid; COT, *Celastrus orbiculatus* Thunb.; COX-2, cyclooxygenase-2; DCA, deoxycholic acid; Gclm, glutamate-cysteine ligase regulatory subunit; Gpx1, glutathione peroxidase 1; GR, glucocorticoid receptor; Gsta, glutathione S-transferase α ; IL-1 β , Interleukin 1 beta; iNOS, cytokine-inducible nitric oxide synthase; i.p., intraperitoneal; LBD, ligand-binding domain; LCA, lithocholic acid; LDH, lactate dehydrogenase; MIP-1 α , macrophage inflammatory protein 1 α ; NCoR, nuclear corepressor; OCA, obeticholic acid; PBC, primary biliary cholangitis; PPAR, peroxisome proliferator-activated receptor; RAR, retinoic acid receptor; ROR, retinoic acid-related orphan receptor; SAR, structure-activity relationship; SRCs, steroid receptor coactivators; TGF β , transforming growth factor beta; TNF α , tumor necrosis factor alpha; Ugt1a1, uridine diphosphate glucuronosyltransferase 1-1.

MOL #109900

Abstract

Farnesoid X receptor (FXR) and G-protein-coupled BA receptor 1 (GPBAR1) are two important bile acid (BA) receptors. As a non-BAs drug template for GPBAR1, none of the natural oleanane-type triterpene has been reported as FXR ligands, despite that FXR and GPBAR1 have similar binding pockets for BAs. Here, we report the natural triterpene hedragonic acid that has been isolated from the stem and root of *Celastrus orbiculatus* Thunb. (COT) as an effective agonist for FXR. Both biochemical AlphaScreen and cell-based reporter assays showed that hedragonic acid regulated the transcriptional activity of FXR. CD spectroscopy further suggested the conformational changes of FXR upon the binding of hedragonic acid. Interestingly, the crystal structure of hedragonic acid-bound FXR revealed a unique binding mode with hedragonic acid occupying a novel binding pocket different from the classical binding position. The structural comparison between hedragonic acid-bound FXR and oleanolic acid-bound GPBAR1 explained the molecular basis for the selectivity of oleanane-type triterpenes for FXR. Moreover, hedragonic acid treatment protected mice from liver injury induced by overdose acetaminophen and decreased hepatic inflammatory responses in an FXR-dependent manner, suggesting that hedragonic acid might be one of the major components of COT for its multifunctional pharmaceutical uses. In conclusion, our results have provided novel structure templates for drug design based on natural triterpenes by targeting FXR and/or GPBAR1 with pharmaceutical values.

MOL #109900

Introduction

Farnesoid X receptor (FXR) and G-protein-coupled BA receptor 1 (GPBAR1) are two important bile acid (BA) receptors. FXR, a member of the nuclear hormone receptor superfamily, is highly expressed in mammalian liver, intestine, kidney and adrenal gland (Makishima et al., 1999; Parks et al., 1999). Small molecules known as ligands play important roles in modulating the activity of nuclear receptors (Benet et al., 2015; McKenna, 2016). Like many other nuclear receptors, the ligand binding induces the conformational change of FXR, leading to the modulation of its transcriptional function through the recruitment or release of specific co-regulators, including coactivators like the steroid receptor coactivators (SRC) family, and corepressors such as the nuclear corepressor (NCoR) (Jin and Li, 2010). As a BA receptor, FXR plays important roles in maintaining bile acid homeostasis (Kong et al., 2012; Matsubara et al., 2013; Sun et al., 2017). Moreover, FXR regulates many physiological functions including metabolism, cancer and liver regeneration (Wagner et al., 2011). Notably, FXR null mice display strong hepatic inflammation and develop spontaneous liver tumors (Wang et al., 2008; Yang et al., 2007). Interestingly, FXR ligands have shown anti-inflammatory activity and liver protective effects by targeting FXR pathway (Bhushan et al., 2013; Lee et al., 2010; Meng et al., 2010). GPBAR1 is the membrane-bound BA receptor (Keitel and Haussinger, 2012; Maruyama et al., 2006) that is also highly expressed in the liver and intestine, as well as in brown adipose tissue and the spleen (Keitel and Haussinger, 2012). Similar to FXR, GPBAR1 plays important roles in regulating energy homeostasis and glucose metabolism (Broeders et al., 2015; Thomas et al., 2009). Activated GPBAR1 induces the production of glucagon-like peptide-1, which in turn modulates

MOL #109900

insulin secretion/sensitivity, glucagon secretion, and β -cell mass (Pellicciari et al., 2009). In addition, binding of BAs with GPBAR1 increases energy expenditure in brown adipose tissue, preventing obesity and insulin resistance (Broeders et al., 2015; Watanabe et al., 2006). Thus, both FXR and GPBAR1 have been promising drug targets for treating a variety of diseases affecting liver, intestine and kidney.

Many natural bile acids, such as cholic acid (CA), chenodeoxycholic acid (CDCA), lithocholic acid (LCA) and deoxycholic acid (DCA), are all ligands for both FXR and GPBAR1 (Porez et al., 2012). However, some BAs or semi-synthetic BA derivatives selectively recognize only FXR or GPBAR1. For example, obeticholic acid (OCA; INT-747; 6-ECDC) and TC-100 (3 α ,7 α ,11 β -Trihydroxy-6 α -ethyl-5 β -cholan-24-oic Acid) are potent FXR agonists (Fiorucci et al., 2009; Pellicciari et al., 2016), INT-777 (S-EMCA) and 23(S)-methylated LCA selectively activate GPBAR1, whereas INT-767 is an agonist for both BA receptors (Fiorucci et al., 2009; Sun et al., 2017; Yu et al., 2015). Aside from BAs, a class of plant natural triterpenes, including betulinic acid, oleanolic acid and ursolic acid, were identified as selective GPBAR1 agonists with physiological functions (Genet et al., 2010; Sato et al., 2007). These natural oleanane-type triterpenes have been non-BAs drug templates for target GPBAR1 (Castellano et al., 2013; Genet et al., 2010). Even though FXR and GPBAR1 have similar binding pockets for BAs, none of the oleanane-type triterpenes have been reported as FXR ligands. In this study, we identified hedragonic acid (24-Nor-3-oxo-12-oleanen-28-oic acid), a natural pentacyclic oleanane-type triterpene that has been isolated from the stem and root of *Celastrus orbiculatus* Thunb. (COT),

MOL #109900

as an effective agonist of nuclear receptor FXR with pharmaceutical potentials.

Materials and Methods

Protein preparation. The human FXR LBD (residues 243-472) was expressed as N-terminal 6×His fusion protein from the expression vector pET24a (Novagen). BL21 (DE3) cells transformed with expression plasmids were grown in LB broth at 25 °C to an OD₆₀₀ of ~1.0 and induced with 0.1 mM isopropyl 1-thio-β-D-galactopyranoside (IPTG) at 16 °C. Cells were harvested and sonicated in 200 mL extraction buffer (20 mM Tris pH 8.0, 150 mM NaCl, 10% glycerol and 25 mM imidazole) per 6 liter of cells. The lysate was centrifuged at 20,000 rpm for 30 min, and the supernatant was loaded on a 5 mL NiSO₄-loaded HiTrap HP column (GE Healthcare). The column was washed with extraction buffer and the protein was eluted with a gradient of 25-500 mM imidazole. The FXR LBD was further purified with a Q-Sepharose column (Amersham Biosciences). To prepare the protein-ligand complex, we added a five-fold molar excess of hedragonic acid to the purified protein, followed by filter concentration to 10 mg/mL. The FXR LBD was complexed with two-fold molar of a SRC2-3 peptide (QEPVSPKKKENALLRYLLDKDDTKD) before filter concentration.

Coregulator Binding Assays. The binding of the various coregulator peptide motifs to FXR LBD in response to ligands was determined by AlphaScreen assays using a hexahistidine detection kit from Perkins-Elmer as described before (Li et al., 2005). The hedragonic acid was purchased from BioBioPha (Yunnan, China), while the rest triterpenes were purchased from

MOL #109900

TargetMol (Shanghai, China). The experiments were conducted with approximately 20-40 nM receptor LBD and 20 nM biotinylated cofactor peptides in the presence of 5 µg/mL donor and acceptor beads in a buffer containing 50 mM MOPS, 50 mM NaF, 0.05 mM CHAPS, and 0.1 mg/mL bovine serum albumin, all adjusted to a pH of 7.4. The peptides with an N-terminal biotinylation are listed as: NCoR-1, QVPRTHRLITLADHICQIITQDFAR; NCoR-2, GHSFADPASNLGLEDIIRKALMGSF; SRC1-2, SPSSHSSLTERHKILHRLQLQEGSP; SRC2-3, QEPVSPKKKENALLRYLLDKDDT KD; SRC3-3, PDAASKHKQLSELLRGGSG.

Circular Dichroism (CD) Spectroscopy. CD measurements were carried out using a Jasco J-8106 spectro-polarimeter (JASCO, Tokyo) as previously described (Zhan et al., 2008). The CD spectra were obtained in 10 mM phosphate buffer (pH 7.4) using a cell with a 0.5-cm path length. FXR LBD protein was dialyzed against phosphate buffer (10 mM phosphate, pH7.4). Gradient concentrations of ligands were added to the protein. After incubation for 2 min at room temperature, the CD spectra were measured.

Dual-Luciferase Reporter assay. HEK-293T cells were maintained in DMEM containing 10% fetal bovine serum and were transiently transfected using Lipofectamine 2000 (Invitrogen). All mutant FXR plasmids were created using the Quick-Change site-directed mutagenesis kit (Stratagene). Before 24 h of transfection, 24-well plates were plated (5×10^4 cells per well). For nuclear receptor luciferase reporter assay, the cells were co-transfected with plasmids encoding full-length nuclear receptors and their cognate luciferase reporters as follows: human FXRα with

MOL #109900

EcRE-Luc, human PPARs (α , δ , and γ) with PPRE-Luc; human RORs (α , β and γ) with the Pcp2/RORE-Luc; human GR or AR with the MMTV-Luc; human RARs with β RE-Luc reporter. For GPBAR1 reporter assay, the cells were co-transfected with plasmids encoding full-length GPBAR1 and pCRE-luc reporter (Yu et al., 2015). Ligands were added 5 h after transfection. Cells were harvested 24 hours later for the luciferase assays with the Dual-Luciferase Reporter assay system (Promega). The luciferase activities were normalized to renilla activity co-transfected as an internal control.

Crystallization and structure determination. The crystal of FXR/hedragonic acid complex was grown at room temperature in hanging drops containing 1.0 μ L of the ligand-protein solutions and 1.0 μ L of well buffer containing 0.1 M HEPES pH 7.5, 10% w/v Polyethylene glycol 6,000, 5% v/v (+/-)-2-Methyl-2,4-pentanediol. The crystals were directly flash frozen in liquid nitrogen for data collection. The observed reflections were reduced, merged and scaled with DENZO and SCALEPACK in the HKL2000 package (Otwinowski and Minor, 1997). The structures were determined by molecular replacement in the CCP4 suite. Manual model building was carried out with Coot (Emsley and Cowtan, 2004), followed by Refmac5 refinement in the CCP4 suite.

Molecular docking. The structure of GPBAR1 for docking was a gift from Prof. Vittorio Limongelli (D'Amore et al., 2014). The docking was carried out using the AutoDock4.2 software package (Huey et al., 2007). Grid points of $65 \times 80 \times 55$ for GPBAR1 with a 0.375 Å spacing calculated around the binding cavity was deemed as the docking site (D'Amore et al., 2014).

MOL #109900

Three dimensional structures of ligands were constructed using the software Discovery Studio (Discovery Studio, version 2.5.5, Accelrys Software Inc. CA, San Diego, 2010) (Accelrys Inc.). Atom types were assigned using the CHARMM force field. Partial charges were added using the Gasteiger algorithm. Energy optimization was carried out to obtain the lowest energy conformation using the steepest descent method under the implicit solvent model with a dielectric constant of 1.0. The visualization was performed using the program Pymol (DeLano Scientific, Palo Alto, CA). Default cutoff values of 4.0 Å for van der Waals (vdW) and 2.5 Å for H-bond interactions were employed. Ten conformations were retained for each ligand. Then the docking run consisted of 10 million energy evaluations using the Lamarckian genetic algorithm local search method. Otherwise default docking parameters were applied.

Animals and treatments. Male mice at 8 weeks of age were maintained under environmentally controlled conditions with free access to standard chow diet and water. Animal experiments were conducted in the barrier facility of the Laboratory Animal Center, Xiamen University, approved by the Institutional Animal Use and Care Committee of Xiamen University, China. Vehicle (40% w/v of 2-hydroxypropyl- β -cyclodextrin) or hedragonic acid (10 mg/kg body weight) dissolved in vehicle were intraperitoneal (i.p.) injected once daily for five days. Six hours after the fifth injection, 500 mg/kg body weight of APAP solved in PBS was i.p. injected to the mice. 24 hours later, mice were sacrificed. Parts of liver tissues were fixed in 4% paraformaldehyde, and the liver histology characterization was analyzed by haematoxylin and eosin (H&E) staining with paraffin-embedded sections by standard procedures. Other liver tissues were collected for

MOL #109900

real-time quantitative reverse transcription PCR (RT-PCR). The serums were collected to measure enzymes activities including lactate dehydrogenase (LDH), alanine aminotransferase (ALT) and aspartate aminotransferase (AST) using commercial kits (Biosino Bio-technology and science inc., Beijing, China; Nanjing Jiancheng Bioengineering Institute, Nanjing, China).

RT-PCR. RNA was isolated using RNA kit (Omega Bio-Tek, GA). The first strand cDNA were obtained by TAKARA reverse transcription kit. Real-time quantitative PCR were performed on a CFX96™ Real-Time PCR Detection System (Bio-Rad) using SYBR Premix Ex Taq™ (TAKARA). Relative mRNA expression levels were normalized to GAPDH levels. The primers used in this assay were listed in the Supplemental Table 1.

Statistical analysis. Results were expressed as mean \pm s.e.m. *P*-values were calculated by using unpaired two-tailed Student's *t*-test. *P* less than 0.05 was considered significant.

Results

Identification of hedragonic acid as a novel FXR agonist. In search of novel modulators for FXR, we used FXR ligand-binding domain (LBD) as a bait to screen natural compounds based on AlphaScreen biochemical assay, which determines the efficacy of small molecules in influencing binding affinity of FXR with co-regulator peptides (Jin et al., 2013). The screen results revealed a natural pentacyclic oleanane-type triterpene, hedragonic acid, potently activated FXR in a concentration dependent manner (Figure 1A). Hedragonic acid induces FXR

MOL #109900

to recruit nuclear receptor coactivator motifs from SRC1, SRC2 and SRC3, but not corepressor motifs from NCoR (Figure 1B), suggesting that hedragonic acid is an agonist of FXR. We further employed CD spectroscopy to detect the secondary structural changes of FXR LBD induced by ligands (Figure 1C & 1D). The results showed that hedragonic acid induced conformational changes of FXR LBD in a similar way to the full agonist GW4064, suggesting the physical interaction of hedragonic acid with FXR. Moreover, cell-based reporter assays further revealed that hedragonic acid selectively activates FXR among many other nuclear receptors tested, but with a relative moderate activity compared to the synthetic agonist GW4064 (Figure 1E). Importantly, hedragonic acid induced the expression of FXR target genes in primary hepatocytes from wild type mice but not FXR knockout mice in a dose-dependent manner, affirming that hedragonic acid is an FXR agonist (Supplemental Figure 1 & 2).

To investigate whether other oleanane-type triterpenes are FXR ligands, asiatic acid, oleanolic acid, 18 β -glycyrrhetic acid, friedelin, ursolic acid and berulinic acid were selected to test their activities on FXR in recruiting coactivators by AlphaScreen assays. Despite high structural similarity among these triterpenes, none of the tested triterpenes except hedragonic acid activated FXR (Figure 1F), demonstrating a highly selective structural recognition of oleanane-type triterpenes by FXR. Interestingly, hedragonic acid showed a weak GPBAR1 activity in cell-based reporter assay (Figure 1G). Structurally compared to other triterpenes, hedragonic acid is characterized with both carbonyl group on one end in the C3 (Supplemental Figure 3), which may play a pivotal role in recognition of the pocket binding sites in FXR.

MOL #109900

Structure determination of the binding mode of hedragonic acid with FXR. To determine the molecular basis of the binding selectivity of hedragonic acid by FXR, we solved the crystal structure of FXR complexed with hedragonic acid (Figure 2, Supplemental Table 2, PDB ID 5wzx). The data statistics and the refined structures are summarized in Supplemental Table 2. The structure of hedragonic acid-bound FXR LBD assumed a dimer form with the arrangement of a three-layer helical sandwich, with hedragonic acid occupying the pocket formed by the helical structure of H3, H9 and H11 (Figure 2A), resulting in an active conformation for FXR. Hedragonic acid was clearly observed to fit in the electron density map as shown in Figure 2B, predominately by hydrophobic interactions with FXR residues of Trp454, Phe329, Met328, Phe366, Leu287, Phe461 and Trp464. In addition, two polar contacts with the C-terminal of helix 10 further anchored the ligand position: one is a 2.39 Å hydrogen bond from His477 to the carbonyl oxygen of hedragonic acid, and the other hydrogen bond is between the NH moiety of Trp454 and a lipid carbonyl group in hedragonic acid with a 2.9 Å distance (Figure 2B). Notably, these two key pharmacophores are unique features of hedragonic acid necessary for its molecular recognition by FXR (Figure 2C), providing a clue in drug design based on the structure of pentacyclic triterpene. Superposition of structures of hedragonic acid-bound FXR with GW4064-bound FXR (PDB ID 3dct) (Akwabi-Ameyaw et al., 2009) and CDCA-bound FXR (PDB ID 4qe6) revealed that hedragonic acid occupies a distinct binding site compared to the classical pocket occupied by GW4064 or CDCA (Figure 2C). The three ligands also exhibited different orientations in the pockets (Figure 2C & 2D).

MOL #109900

Due to the unique binding site of hedragonic acid in FXR, hedragonic acid induces series of conformational changes of FXR LBD (Figure 3). Specifically, the loss of classical hydrogen bond interaction with Arg331 and the unoccupied space around the Phe336 induced the helix 5, 3 and 7 inwardly squeezed, leading to the reduction of FXR pocket size (Figure 3A). In addition, hedragonic acid binding also induced the conformational changes of internal hydrophobic residues of FXR, including Trp454, Phe461 and Tyr369 in comparison to GW4064- or CDCA-bound FXR LBD (Figure 3B-3D). Thus, hedragonic acid initiates a hydrophobic interaction between its methyl groups and the benzene ring of FXR Tyr369, in addition to a key hydrogen bond interaction with FXR Trp454, which further echoes the formation of the unique binding pocket of FXR by hedragonic acid. Notably, the retained hydrogen bond between the carbonyl oxygen of hedragonic acid and the NH moiety in His447 might also play an important role in maintaining the active state of FXR (Figure 3D), which stabilizes the protein conformation that is capable of recruiting co-activators (Jin et al., 2013).

Structural validation by mutagenesis assays. To validate the roles of the critical residues in the hedragonic acid binding pocket, the site-directed mutagenesis was employed to test the transcriptional activity of FXR in response to hedragonic acid in cell-based reporter assays. A291W mutation was designed to cause a sharp reduction on the size of FXR pocket through the enlargement of the corresponding side chain in the ligand binding pocket (Figure 4A & 4B). As expected, a dramatic abolishment in the FXR transcriptional activity by GW4064, CDCA and hedragonic acid was observed in this mutated FXR (Figure 4D). The H447F mutant was

MOL #109900

constructed to destroy the hydrogen bonds between His447 and hedragonic acid or CDCA, which are the key interaction in their binding mode (Figure 4A & 4C). Correspondingly, H447F resulted in the vanished FXR transcriptional induction by hedragonic acid and CDCA, respectively (Figure 4D). Considering the unique polar distribution of the residues around the hedragonic acid binding pocket, three mutants of L287T, T288V and F284Y were chosen to evaluate the effect of the polar changes on the specificity of pocket binding site. Specifically, the L287T was located in the overlapped binding site of the three ligands in their binding pockets. This mutant changed the favorable hydrophobic environment in the ligand binding pocket as it occupied a vital position forming hydrophobic interactions with the lipid and bulky steric moiety of ligands (Figure 4A). Accordingly, the transcriptional activity of FXR with L287T mutation was abolished by all the three ligands (Figure 4D). In contrast, Thr288 and Phe284 only participated in the binding pocket of hedragonic acid. The lack of a hydroxyl side chain in the T288V mutant weakened electrostatic interactions of FXR with the carbonyl group of hedragonic acid, leading to a moderate decline in the transcriptional activity of FXR by hedragonic acid. In contrast, no changes in the transcriptional activity by GW4064 and CDCA were observed in this mutant. Based on our solved structure, a putative hydrogen bond was predicted to emerge between hedragonic acid and the mutant F284Y, due to the hydroxyl group of tyrosine as a hydrogen bond donor in the interaction with hedragonic acid. As expected, the FXR transactivation of this mutant was significantly enhanced by hedragonic acid (Figure 4D), but with a relatively modest impact on the function of CDCA and GW4064. These results further validated the unique binding mode of hedragonic acid with FXR.

MOL #109900

Structural comparison of ligands binding to FXR and GPBAR1. The obvious difference between hydrogonic acid and oleanolic acid is apparent with the ketone for hydrogonic acid and the hydroxyl group for oleanolic acid, respectively, at position C-3 (Supplemental Figure 3), which may dictate the differential binding affinity of oleanane-type triterpenes to FXR and GPBAR1. If the ketone of hydrogonic acid is replaced with a hydroxyl group, the volume of Van der Waals and polar molecular surface would increase in this orientation of the FXR pocket (Supplemental Figure 4 and Supplemental Table 3). In the ligand binding pocket of FXR, the cavity formed by key residues of Phe461, Trp454 and Leu287 offers a relative narrow and hydrophobic space for ligand binding with a 3.1 Å distance between the ketone oxygen atom to the C1 atom of aromatic face (pi system) in Trp454 (Figure 5A, Supplemental Figure 4), which acts as a critical factor for the preference of hydrogonic acid from the oleanane-type triterpenes for FXR.

To further investigate the structural mechanism of the binding specificity of oleanane-type triterpenes to FXR and GPBAR1, we compared the two binding modes of the crystal structure of hydrogonic acid with FXR and the docking model of oleanic acid with GPBAR1 using AutoDock4.2 (AD4.2) (Figure 5). The docking simulations on the GPBAR1 in complex with oleanolic acid showed that the oleanolic acid occupies the binding site of GPBAR1 by more polar interactions than hydrogonic acid in FXR (Figure 5B, F). In particular, oleanolic acid occupies the cavity formed by TM2, TM3, TM5 and TM7, with its oleanane-type triterpenoid scaffold forming favorable interactions with the side chains of Glu169, Tyr240, Phe96, Leu68 and Ser270

MOL #109900

(Figure 5B). Moreover, the hydroxyl group in C-3 moiety of oleanolic acid extends to the inside position of the hydrophobic cavity formed by Leu24, Leu68 and Trp237, establishing a key hydrogen bond interaction with Ser270 (Figure 5B & 5D). Whereas, this key hydrogen bond might be unavailable if the C-3 position changes to the ketone of hedragonic acid, resulting in a weaker activity to GPBAR1. Also, compared to oleanolic acid, hedragonic acid is characterized by the methyl group at C-4. The steric properties of the exocyclic methyl and triterpenoid are important determinants to bind the different shapes of lipophilic pockets. In complex with FXR, the single methyl group at C-4 of hedragonic acid favors its interaction through a cation- π interaction with Trp454 with less steric effects (Figure 5C & 5E). However, more hydrophobic interactions are acquired for the two methyl groups at C-4 of oleanolic acid when it binds to GPBAR1 (Figure 6B). Thus, the hydroxyl group and ketone at position C-3 and the steric hindrance of the adjacent groups in the scaffold of triterpenoid determine the preference or selectivity of hedragonic acid and oleanolic acid to FXR and GPBAR1, respectively.

To further elucidate the differential binding modes between oleanolic acid and hedragonic acid to GPBAR1, we mutated several key residues that contribute to the ligand interaction, and then tested the activity of these mutated GPBAR1 in response to oleanolic acid and hedragonic acid in cell based reporter assays. The mutations Y89F and E169A were predicted to damage the polar interaction of ligands (Figure 5B, Supplemental Figure 5), and the A67W and L71T mutations were designed to destroy the hydrophobic environment for ligand binding (Figure 5D, Supplemental Figure 5). As expected, these mutations substantially reduced GPBAR1 activities

MOL #109900

mediated by both oleanolic acid and hedragonic acid (Supplemental Figure 5). The S270A mutation was designed to abolish the hydrogen bond between oleanolic acid and GPBAR1. As expected, S270A substantially decreased the activity of GPBAR1 regulated by oleanolic acid, but not by hedragonic acid (Supplemental Figure 5). These results further affirm the ligand-binding pocket of GPBAR1 simulated by molecular docking, and highlight the differential roles of GPBAR1 transmembrane residues in recognizing various ligands.

Hedragonic acid showed therapeutic effects on liver injury and inflammation dependent on FXR. FXR mediated by ligands plays important roles in liver protection. To investigate the effects of hedragonic acid in liver injury, APAP induced liver injury was used as a mouse model. After being administrated with hedragonic acid (10 mg/kg) for 5 days, mice were i.p. injected with a single challenge of APAP (500 mg/kg). 24 hours later, liver sections and activities of liver enzymes were examined. H&E-stained liver sections showed that hedragonic acid pretreatment maintained the liver morphological characteristics compared with the hepatocytes injury shown in vehicle-treated control (Figure 6A & 6B). Consistently, serum levels of LDH, ALT and AST were significantly lower in the hedragonic acid treated mice compared with those in the vehicle-treated mice (Figure 6C). It has been reported that activated FXR by ligands could induce several genes involved in xenobiotic metabolism (Lee et al., 2010). We then monitored the mRNA levels of glutathione S-transferase $\alpha 3$ (Gsta3) and Gsta4, GSH metabolism-related genes (Gclm and Gpx1), and glucuronosyltransferase (Ugt1a1) in the liver samples of the mice. The results showed that hedragonic acid treatment significantly induced the expression of these genes

MOL #109900

(Figure 6D). Overdose of APAP caused liver injury also displays liver inflammation due to the increased activities of AST, ALT and LDH. Hedragonic acid treatment also decreased the mRNA levels of inflammatory genes including iNOS, TGF β , TNF α , COX-2, IL-1 β and MIP-1 α in liver samples of the mice challenged with overdose APAP (Figure 6E). These results demonstrate that administration of hedragonic acid could provide protection from APAP-induced liver injury and inflammation.

To investigate whether the liver protection effects of hedragonic acid is dependent on FXR, primary hepatocytes were isolated from wild-type (WT) and FXR knock-out (KO) mice, respectively. After pretreatment with hedragonic acid for 18 hours, 20 μ g/ml of LPS was administrated to the cells. The mRNA levels of the inflammatory genes were measured 6 hours later. The results showed that hedragonic acid significantly decreased the mRNA level of TNF α and IL-1 β in LPS-treated primary hepatocytes from wild type mice but not in the hepatocytes from FXR KO mice (Figure 6F), indicating that hedragonic acid elicits its anti-inflammatory responses by targeting FXR.

Discussion

Dual or selective FXR and/or GPBAR1 agonists are prevailing strategies in drug discovery for enterohepatic and metabolic disorders (Fiorucci et al., 2009). As endogenous ligands, BAs provide promising templates for structure-based drug design and development. So far, however, only OCA, that is derived from CDCA, has been approved for clinical use for the treatment of

MOL #109900

primary biliary cholangitis (PBC). Notwithstanding that the phase II FLINT trial results demonstrated that OCA is a potential therapy for the NASH patient population with diabetes, the severe side effects, including jaundice, worsening ascites, PBC, reduction in HDL-C, increment in LDL-C and especially severe pruritus, still exist to limit its clinical usage. Therefore, exploring non-BAs agonists for FXR or GPBAR1 might point to a potential direction in drug development by targeting BA receptors. Since series of natural triterpenes have been identified as GPBAR1 agonists, the triterpenes have become promising lead compounds for drug design by targeting GPBAR1. However, it remains unclear why these triterpenes selectively recognize GPBAR1, but not FXR, even though FXR and GPBAR1 share similar binding pockets for BAs. In this study, we identified the natural triterpene hedragonic acid as a first oleanane-type triterpene FXR agonist. The crystal structure of hedragonic acid in complex with FXR reveals a unique binding mode with hedragonic acid occupying an unclassical binding site. Structural comparison shed light on the molecular selectivity of similar oleanane-type triterpenes to their preferred receptors FXR or GPBAR1. In vivo and in vitro studies demonstrate that hedragonic acid exerts its physiological functions dependent on FXR. These results provide novel evidences for drug design based on natural triterpenes by targeting FXR and/or GPBAR1.

With a great variety of structural compounds, natural products from the herbal medicine are an extremely productive source for new medicines or lead compounds for drug discovery and development (Koehn and Carter, 2005). COT is a woody vine of the *Celastraceae* family, which is widely distributed in Eastern Asia and also North America (Hou, 1955). As a traditional

MOL #109900

Chinese medicinal herb, the extracts from the stem and root of COT have been used as a remedy against swelling, pain, rheumatoid arthritis, bruises, amenorrhea, vomiting, limbs numbness, hepatitis, Jaundice hepatitis and cancer (Group, 1999; Wang et al., 2012). It has been reported that compounds isolated from COT show specific pharmacological functions (Li et al., 2016; Yang et al., 2006; Zhang et al., 2016). However, since numerous and complex compositions exist in the plant extracts, the mechanism of the multifunctional COT remains unclear. Hedragonic acid is one of the main components of COT (Li, 2012) and is here identified as an agonist of nuclear receptor FXR with effective liver protection and anti-inflammatory activity. Considering the important roles of FXR in physiology and pathology, these results suggest that hedragonic acid might be one of the major components of COT for its pharmaceutical uses by targeting FXR.

MOL #109900

Acknowledgements

We thank the staff at BL17U of the Shanghai Synchrotron Radiation Source for assistance in data collection. The model of GPBAR1 is a kind gift from Professor Vittorio Limongelli. We also thank Professor Tao Lu for offering the usage of soft wares for molecular docking.

Authorship Contributions

Participated in research design: L. Jin, Li.

Conducted experiments: Zheng, Lin, Guo, Zhu, Wei, Liu, S. Jin, L. Jin, Li.

Performed data analysis: Lu, L. Jin, Li.

Wrote or contributed to the writing of the manuscript: Lu, L. Jin, Li.

Notes

The authors declare no competing financial interest.

References

- Akwabi-Ameyaw A, Bass JY, Caldwell RD, Caravella JA, Chen L, Creech KL, Deaton DN, Madauss KP, Marr HB, McFadyen RB, Miller AB, Navas F, 3rd, Parks DJ, Spearing PK, Todd D, Williams SP and Bruce Wisely G (2009) FXR agonist activity of conformationally constrained analogs of GW 4064. *Bioorganic & medicinal chemistry letters* **19**(16): 4733-4739.
- Benet M, Guzman C, Pisonero-Vaquero S, Garcia-Mediavilla MV, Sanchez-Campos S, Martinez-Chantar ML, Donato MT, Castell JV and Jover R (2015) Repression of the nuclear receptor small heterodimer partner by steatotic drugs and in advanced nonalcoholic fatty liver disease. *Molecular pharmacology* **87**(4): 582-594.
- Bhushan B, Borude P, Edwards G, Walesky C, Cleveland J, Li F, Ma X and Apte U (2013) Role of bile acids in liver injury and regeneration following acetaminophen overdose. *The American journal of pathology* **183**(5): 1518-1526.
- Broeders EP, Nascimento EB, Havekes B, Brans B, Roumans KH, Tailleux A, Schaart G, Kouach M, Charton J, Deprez B, Bouvy ND, Mottaghy F, Staels B, van Marken Lichtenbelt WD and Schrauwen P (2015) The Bile Acid Chenodeoxycholic Acid Increases Human Brown Adipose Tissue Activity. *Cell metabolism* **22**(3): 418-426.
- Castellano JM, Guinda A, Delgado T, Rada M and Cayuela JA (2013) Biochemical basis of the antidiabetic activity of oleanolic acid and related pentacyclic triterpenes. *Diabetes* **62**(6): 1791-1799.
- D'Amore C, Di Leva FS, Sepe V, Renga B, Del Gaudio C, D'Auria MV, Zampella A, Fiorucci S and Limongelli V (2014) Design, synthesis, and biological evaluation of potent dual agonists of nuclear and membrane bile acid receptors. *Journal of medicinal chemistry* **57**(3): 937-954.
- Emsley P and Cowtan K (2004) Coot: model-building tools for molecular graphics. *Acta crystallographica Section D, Biological crystallography* **60**(Pt 12 Pt 1): 2126-2132.
- Fiorucci S, Mencarelli A, Palladino G and Cipriani S (2009) Bile-acid-activated receptors: targeting TGR5 and farnesoid-X-receptor in lipid and glucose disorders. *Trends in pharmacological sciences* **30**(11): 570-580.
- Genet C, Strehle A, Schmidt C, Boudjelal G, Lobstein A, Schoonjans K, Souchet M, Auwerx J, Saladin R and Wagner A (2010) Structure-activity relationship study of betulinic acid, a novel and selective TGR5 agonist, and its synthetic derivatives: potential impact in diabetes. *Journal of medicinal chemistry* **53**(1): 178-190.
- Group CmDW (1999) Chinese medicine Dictionary. *Beijing: Chinese Medical Science and Technology Press* **2**: 1345-1346.
- Hou D (1955) A revision of the genus *Celastrus*. *Annals of the Missouri Botanical Garden* **42**: 8.
- Huey R, Morris GM, Olson AJ and Goodsell DS (2007) A semiempirical free energy force field with charge-based desolvation. *Journal of computational chemistry* **28**(6): 1145-1152.
- Jin L, Feng X, Rong H, Pan Z, Inaba Y, Qiu L, Zheng W, Lin S, Wang R, Wang Z, Wang S, Liu H, Li S, Xie W and Li Y (2013) The antiparasitic drug ivermectin is a novel FXR ligand that regulates metabolism. *Nature communications* **4**: 1937.
- Jin L and Li Y (2010) Structural and functional insights into nuclear receptor signaling. *Advanced drug delivery reviews* **62**(13): 1218-1226.
- Keitel V and Haussinger D (2012) Perspective: TGR5 (Gpbar-1) in liver physiology and disease. *Clinics and research in hepatology and gastroenterology* **36**(5): 412-419.
- Koehn FE and Carter GT (2005) The evolving role of natural products in drug discovery. *Nature reviews Drug discovery* **4**(3): 206-220.

MOL #109900

- Kong B, Wang L, Chiang JY, Zhang Y, Klaassen CD and Guo GL (2012) Mechanism of tissue-specific farnesoid X receptor in suppressing the expression of genes in bile-acid synthesis in mice. *Hepatology* **56**(3): 1034-1043.
- Lee FY, de Aguiar Vallim TQ, Chong HK, Zhang Y, Liu Y, Jones SA, Osborne TF and Edwards PA (2010) Activation of the farnesoid X receptor provides protection against acetaminophen-induced hepatic toxicity. *Molecular endocrinology* **24**(8): 1626-1636.
- Li H, Li J, Liu L, Zhang Y, Luo Y, Zhang X, Yang P, Zhang M, Yu W and Qu S (2016) Elucidation of the Intestinal Absorption Mechanism of Celastrol Using the Caco-2 Cell Transwell Model. *Planta medica* **82**(13): 1202-1207.
- Li J, Yang, J., Lu, F., Qi, Y., Liu, Y., Sun, Y., Wang, Q. (2012) Chemical constituents from the stems of *Celastrus orbiculatus*. *Chinese Journal of Natural Medicines* **10**(4): 0279-0283.
- Li Y, Choi M, Cavey G, Daugherty J, Suino K, Kovach A, Bingham NC, Kliewer SA and Xu HE (2005) Crystallographic identification and functional characterization of phospholipids as ligands for the orphan nuclear receptor steroidogenic factor-1. *Molecular cell* **17**(4): 491-502.
- Makishima M, Okamoto AY, Repa JJ, Tu H, Learned RM, Luk A, Hull MV, Lustig KD, Mangelsdorf DJ and Shan B (1999) Identification of a nuclear receptor for bile acids. *Science* **284**(5418): 1362-1365.
- Maruyama T, Tanaka K, Suzuki J, Miyoshi H, Harada N, Nakamura T, Miyamoto Y, Kanatani A and Tamai Y (2006) Targeted disruption of G protein-coupled bile acid receptor 1 (Gpbar1/M-Bar) in mice. *The Journal of endocrinology* **191**(1): 197-205.
- Matsubara T, Li F and Gonzalez FJ (2013) FXR signaling in the enterohepatic system. *Molecular and cellular endocrinology* **368**(1-2): 17-29.
- McKenna NJ (2016) Research Resources for Nuclear Receptor Signaling Pathways. *Molecular pharmacology* **90**(2): 153-159.
- Meng Z, Wang Y, Wang L, Jin W, Liu N, Pan H, Liu L, Wagman L, Forman BM and Huang W (2010) FXR regulates liver repair after CCl₄-induced toxic injury. *Molecular endocrinology* **24**(5): 886-897.
- Otwinowski Z and Minor W (1997) Processing of X-ray diffraction data collected in oscillation mode. *Methods in enzymology* **276**: 307-326.
- Parks DJ, Blanchard SG, Bledsoe RK, Chandra G, Consler TG, Kliewer SA, Stimmel JB, Willson TM, Zavacki AM, Moore DD and Lehmann JM (1999) Bile acids: natural ligands for an orphan nuclear receptor. *Science* **284**(5418): 1365-1368.
- Pellicciari R, Gioiello A, Macchiarulo A, Thomas C, Rosatelli E, Natalini B, Sardella R, Pruzanski M, Roda A, Pastorini E, Schoonjans K and Auwerx J (2009) Discovery of 6alpha-ethyl-23(S)-methylcholic acid (S-EMCA, INT-777) as a potent and selective agonist for the TGR5 receptor, a novel target for diabetes. *Journal of medicinal chemistry* **52**(24): 7958-7961.
- Pellicciari R, Passeri D, De Franco F, Mostarda S, Filipponi P, Colliva C, Gadaleta RM, Franco P, Carotti A, Macchiarulo A, Roda A, Moschetta A and Gioiello A (2016) Discovery of 3alpha,7alpha,11beta-Trihydroxy-6alpha-ethyl-5beta-cholan-24-oic Acid (TC-100), a Novel Bile Acid as Potent and Highly Selective FXR Agonist for Enterohepatic Disorders. *Journal of medicinal chemistry*.
- Porez G, Prawitt J, Gross B and Staels B (2012) Bile acid receptors as targets for the treatment of dyslipidemia and cardiovascular disease. *Journal of lipid research* **53**(9): 1723-1737.
- Sato H, Genet C, Strehle A, Thomas C, Lobstein A, Wagner A, Mioskowski C, Auwerx J and Saladin R (2007)

MOL #109900

- Anti-hyperglycemic activity of a TGR5 agonist isolated from *Olea europaea*. *Biochemical and biophysical research communications* **362**(4): 793-798.
- Sun R, Yang N, Kong B, Cao B, Feng D, Yu X, Ge C, Huang J, Shen J, Wang P, Feng S, Fei F, Guo J, He J, Aa N, Chen Q, Pan Y, Schumacher JD, Yang CS, Guo GL, Aa J and Wang G (2017) Orally Administered Berberine Modulates Hepatic Lipid Metabolism by Altering Microbial Bile Acid Metabolism and the Intestinal FXR Signaling Pathway. *Molecular pharmacology* **91**(2): 110-122.
- Thomas C, Gioiello A, Noriega L, Strehle A, Oury J, Rizzo G, Macchiarulo A, Yamamoto H, Matak C, Pruzanski M, Pellicciari R, Auwerx J and Schoonjans K (2009) TGR5-mediated bile acid sensing controls glucose homeostasis. *Cell metabolism* **10**(3): 167-177.
- Wagner M, Zollner G and Trauner M (2011) Nuclear receptors in liver disease. *Hepatology* **53**(3): 1023-1034.
- Wang M, Zhang X, Xiong X, Yang Z, Sun Y, Yang Z, Hoffman RM and Liu Y (2012) Efficacy of the Chinese traditional medicinal herb *Celastrus orbiculatus* Thunb on human hepatocellular carcinoma in an orthotopic fluorescent nude mouse model. *Anticancer research* **32**(4): 1213-1220.
- Wang YD, Chen WD, Wang M, Yu D, Forman BM and Huang W (2008) Farnesoid X receptor antagonizes nuclear factor kappaB in hepatic inflammatory response. *Hepatology* **48**(5): 1632-1643.
- Watanabe M, Houten SM, Matak C, Christoffolete MA, Kim BW, Sato H, Messaddeq N, Harney JW, Ezaki O, Kodama T, Schoonjans K, Bianco AC and Auwerx J (2006) Bile acids induce energy expenditure by promoting intracellular thyroid hormone activation. *Nature* **439**(7075): 484-489.
- Yang F, Huang X, Yi T, Yen Y, Moore DD and Huang W (2007) Spontaneous development of liver tumors in the absence of the bile acid receptor farnesoid X receptor. *Cancer research* **67**(3): 863-867.
- Yang H, Chen D, Cui QC, Yuan X and Dou QP (2006) Celastrol, a triterpene extracted from the Chinese "Thunder of God Vine," is a potent proteasome inhibitor and suppresses human prostate cancer growth in nude mice. *Cancer research* **66**(9): 4758-4765.
- Yu DD, Sousa KM, Mattern DL, Wagner J, Fu X, Vaidehi N, Forman BM and Huang W (2015) Stereoselective synthesis, biological evaluation, and modeling of novel bile acid-derived G-protein coupled bile acid receptor 1 (GP-BAR1, TGR5) agonists. *Bioorganic & medicinal chemistry* **23**(7): 1613-1628.
- Zhan Y, Du X, Chen H, Liu J, Zhao B, Huang D, Li G, Xu Q, Zhang M, Weimer BC, Chen D, Cheng Z, Zhang L, Li Q, Li S, Zheng Z, Song S, Huang Y, Ye Z, Su W, Lin SC, Shen Y and Wu Q (2008) Cytosporone B is an agonist for nuclear orphan receptor Nur77. *Nature chemical biology* **4**(9): 548-556.
- Zhang Y, Si Y, Zhai L, Guo S, Zhao J, Sang H, Pang X, Zhang X, Chen A and Qin S (2016) *Celastrus Orbiculatus* Thunb. Reduces Lipid Accumulation by Promoting Reverse Cholesterol Transport in Hyperlipidemic Mice. *Lipids* **51**(6): 677-692.

MOL #109900

Footnotes

This work was supported by grants from the National Natural Science Foundation of China [U1405220, 81471084, 81773793, 31770814 and 31470726]; the Fundamental Research Funds for the Central Universities [20720150052]; the Programme of Introducing Talents of Discipline to Universities [B12001] and the National Science Foundation of China for Fostering Talents in Basic Research [J1310027].

Figure Legends

Figure 1. Identification of natural triterpene hedragonic acid as a novel FXR agonist. (A)

Dose responses of compounds in inducing FXR to recruit SRC1-2 co-regulator binding motif by AlphaScreen assay. (B) Various co-regulator binding motifs bind to FXR in response to 1 μ M hedragonic acid or GW4064 by AlphaScreen assay. The peptide sequences are listed in Experimental Section. (C-D) Compounds physically bind to the ligand binding domain of FXR by CD spectroscopy assay. (E) Receptor-specific transactivation by hedragonic acid. HEK-293T cells were co-transfected with plasmids encoding full-length nuclear receptors and their cognate response reporters, respectively (see Experimental Section). After transfection, cells were treated with dimethyl sulphoxide (DMSO), 1 μ M hedragonic acid or ligands specific for each receptor: FXR, 0.5 μ M GW4064; peroxisome proliferator-activated receptor (PPAR) α , 1 μ M GW590735; PPAR δ , 1 μ M GW0472; PPAR γ , 1 μ M rosiglitazone; AR, 0.1 μ M dihydrotestosterone; GR, 0.1 μ M dexamethasone; RAR α and RAR β , 1 μ M all-trans-retinoic acid. Data were normalized to renilla activity co-transfected as an internal control. Values are the means \pm s.e.m. of three independent experiments. (F) FXR selectively recognized hedragonic acid from various natural triterpenes to recruit SRC1-2 by AlphaScreen assay, * $p < 0.001$ versus vehicle control, n.s., no significance (Student's *t*-test). (G) The GPBAR1 activities of compounds (5 μ M) by reporter assay, * $p < 0.01$ versus vehicle control (Student's *t*-test). Values are the means \pm s.e.m. of three independent experiments.

MOL #109900

Figure 2. Structural determination of the FXR LBD in complex with hedragonic acid. (A)

The dimer structure of FXR LBD bound with hedragonic acid in ribbon representation. FXR LBD is in light green and the SRC2-3 motif is in orange. The bound hedragonic acid is shown in stick representation with carbon and oxygen atoms depicted in cyan and red, respectively. (B) 2Fo-Fc electron density map (1.0σ) showing the bound hedragonic acid in FXR LBD. (C) Specific location of herdragonic acid in the binding pocket. The unique binding pocket of hedragonic acid is shown in dashed black circle, and the classical binding pocket is shown in dashed yellow circle. (D) Superposition of hedragonic acid (cyan) with GW4064 (orange) and CDCA (purple).

Figure 3. Conformational changes of FXR LBD induced by ligand binding. Superposition of the FXR/hedragonic acid structure (FXR is in light green and hedragonic acid is in cyan) with the FXR/GW4064 structure (PDB ID 3dct, FXR is in dark green and GW4064 is in orange) and FXR/CDCA (PDB ID 4eq6, FXR is in white and CDCA is in purple). (A) Hedragonic acid binding to FXR reduced the pocket size formed by helix 5, 3 and 7 compared to GW4064 or CDCA. (B-D) Conformational changes of indicated amino acids induced by ligand binding. The conformational changes and hydrogen bonds are shown using dashed arrows and lines, respectively.

Figure 4. Functional correlation of the hedragonic acid and FXR interactions. (A-C)

Superposition of the FXR/hedragonic acid structure (FXR is in light green) with the

MOL #109900

FXR/GW4064 structure (PDB ID 3dct, FXR is in dark green and the GW4064 is in orange) and FXR/CDCA (PDB ID 4eq6, FXR is in white and CDCA is in purple). The dashed lines indicate the hydrogen bond interaction between His447 and hedragonic acid, and the mutations of A291W and T288V are shown in dashed black circle and dashed grey circle, respectively. (D) Different effects of mutations of key FXR residues on its transcriptional activity in response to hedragonic acid, GW4064 and CDCA in cell-based reporter assays. HEK-293T cells were co-transfected with plasmids encoding full-length wild-type (WT) FXR or FXR mutants as indicated in the figure, together with an EcRE luciferase reporter. The cells were treated with 1 μ M hedragonic acid, 0.5 μ M GW4064 and 1 μ M CDCA, respectively. Values are the means \pm s.e.m. of three independent experiments.

Figure 5. Structural comparison of ligands binding to FXR and GPBAR1. (A) The crystal structure of hedragonic acid bound with FXR LBD in ribbon representation. FXR LBD is in light green and hedragonic acid is in light blue. (B) The docking model of oleanolic acid binding to GPBAR1. GPBAR1 is in grey and oleanolic acid is in pink. The selective positions are marked by dashed circle. (C-D) Detailed information of binding pocket of FXR bound with hedragonic acid (C) and GPBAR1 bound with oleanolic acid (D). The dashed lines indicate the hydrogen bond interaction between Ser270 and oleanolic acid. (E-F) Schematic representation of FXR-hedragonic acid (E) and GPBAR1-oleanolic acid (F) interactions. The polar residues around binding pocket are indicated in orange, and the non-polar ones are in light green. Hydrogen bond interactions are indicated by arrows, and the cation- π interaction is marked by symbols.

Figure 6. Hedragonic acid treatment protected liver from injury and alleviated hepatic inflammation induced by APAP. 8-week-old wild-type mice (4-6 mice per group) were pretreated with vehicle or hedragonic acid (10 mg/kg) once daily for 5 days as described in Experimental Section. Mice were challenged with one dose of 500 mg/kg APAP after the 5th administration of hedragonic acid, and then were sacrificed 24 hours later. (A-B) Representative pictures of H&E-stained paraffin-embedded liver sections from mice treated by vehicle (A) and hedragonic acid (B). (C) Serum levels of ALT, AST, and LDH. (D) hepatic mRNA levels of genes involved in xenobiotic metabolism by RT-PCR. (E) mRNA levels of inflammatory genes in liver tissues of mice. For C-E, * $p < 0.05$, ** $p < 0.01$, *** $p < 0.001$ versus vehicle control (Student's t -test). (F) The primary hepatocytes from wild type (WT) and FXR knockout (KO) mice were pretreated with 5 μ M hedragonic acid for 18 hours before treatment with LPS (20 μ g/mL) for 6 hours. The relative mRNA levels of IL-1 β and TNF α were monitored by RT-PCR. * $p < 0.05$ versus DMSO+LPS control (Student's t -test). Values are the means \pm s.e.m. of three independent experiments.

Figure 1

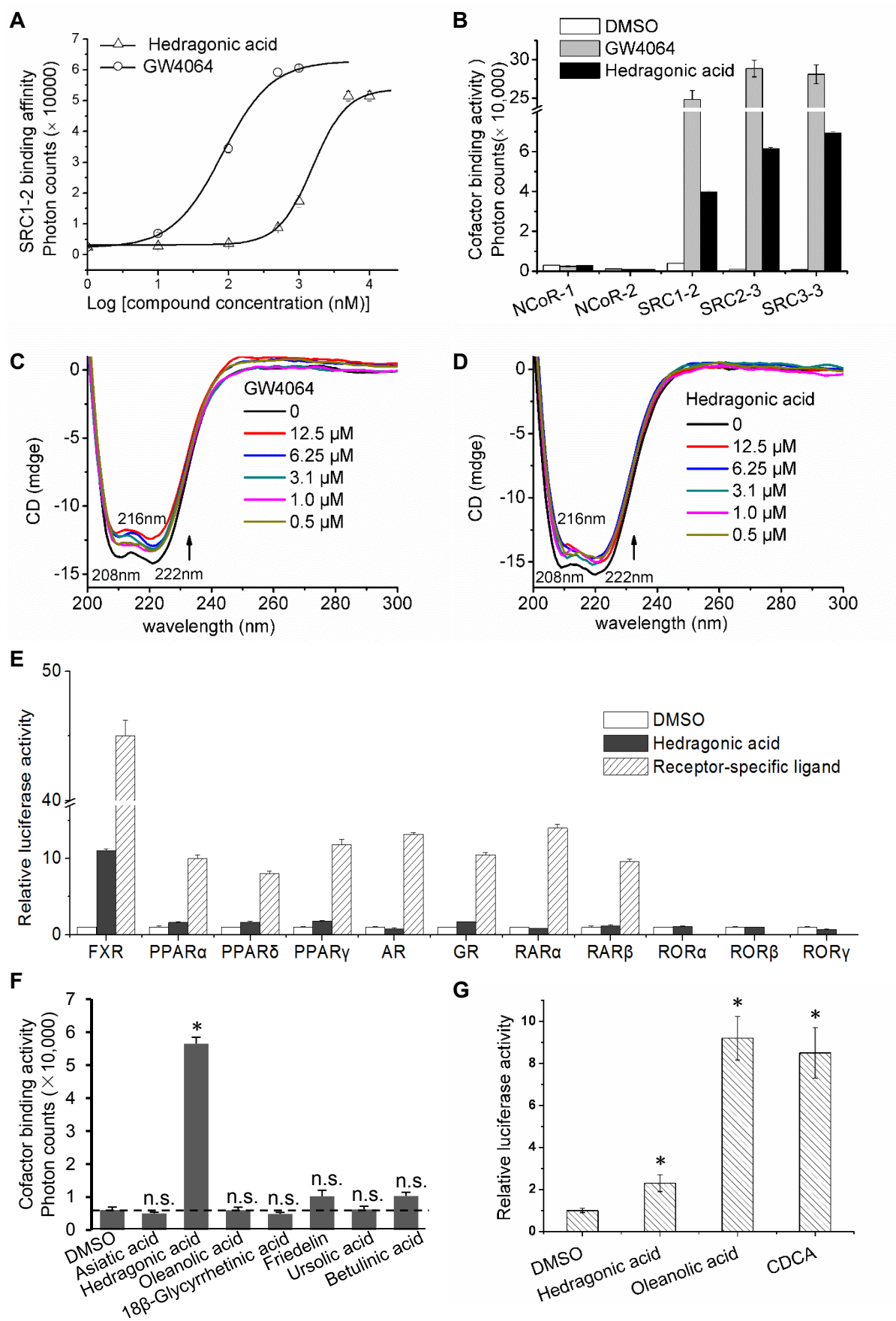


Figure 2

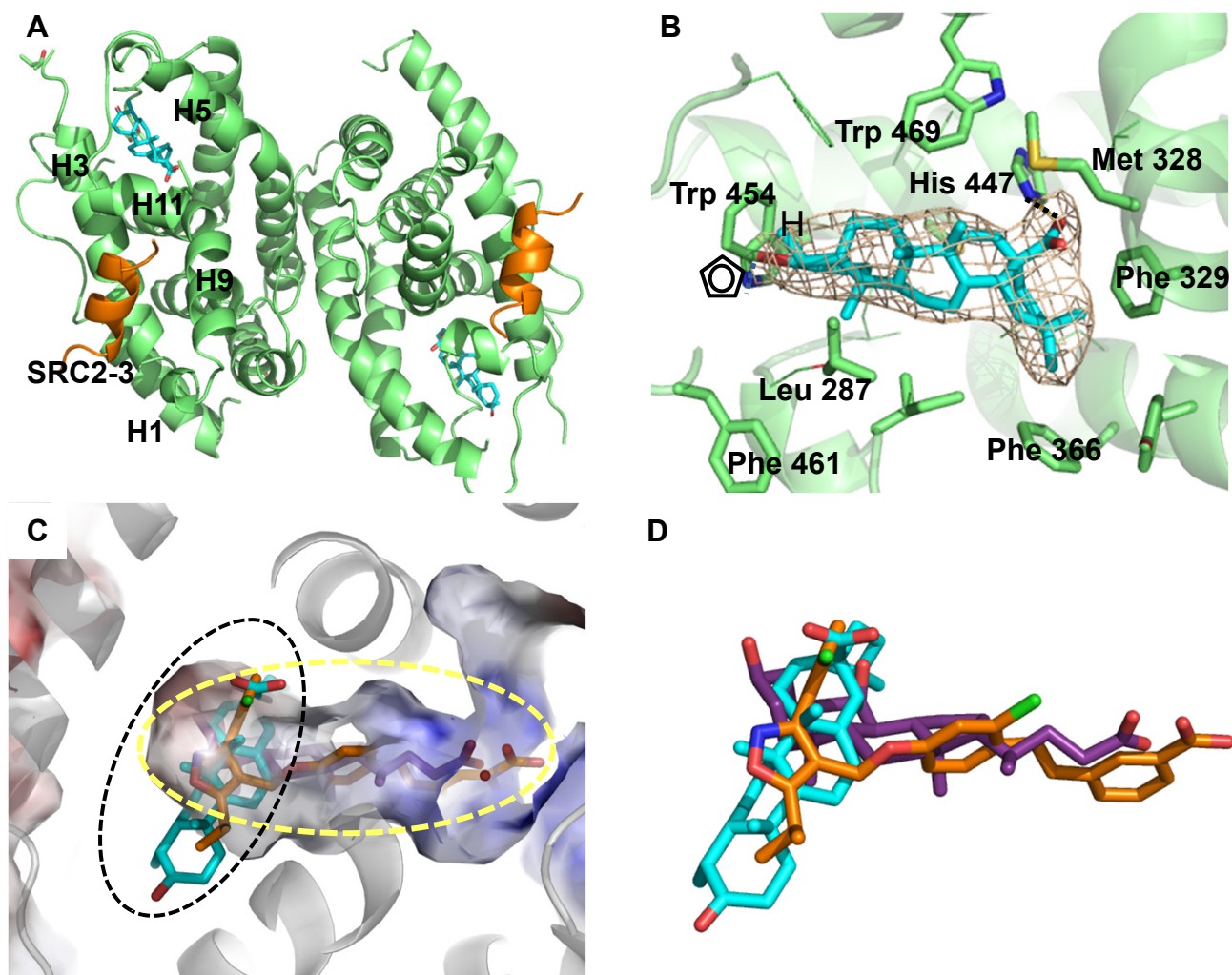


Figure 3

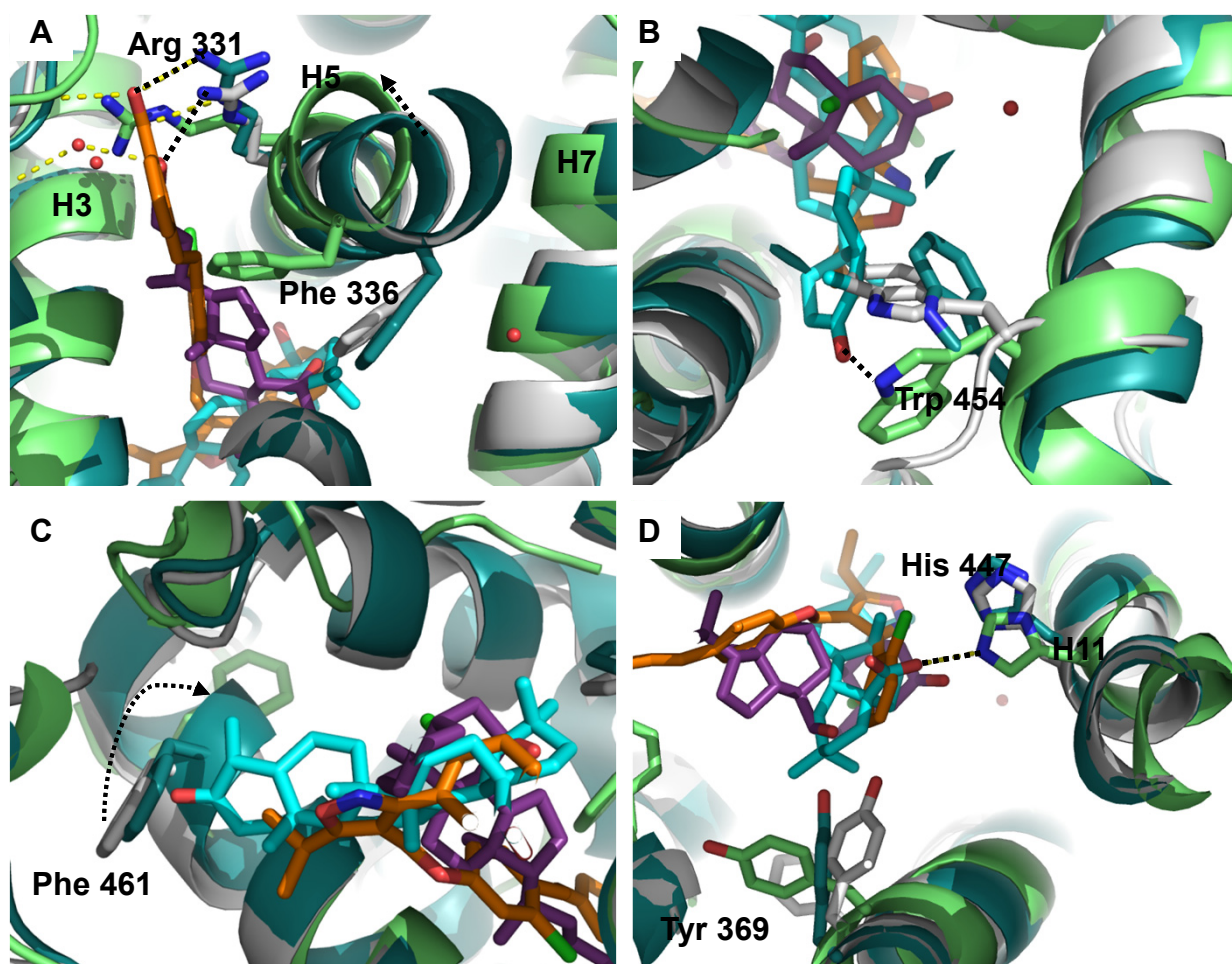


Figure 4

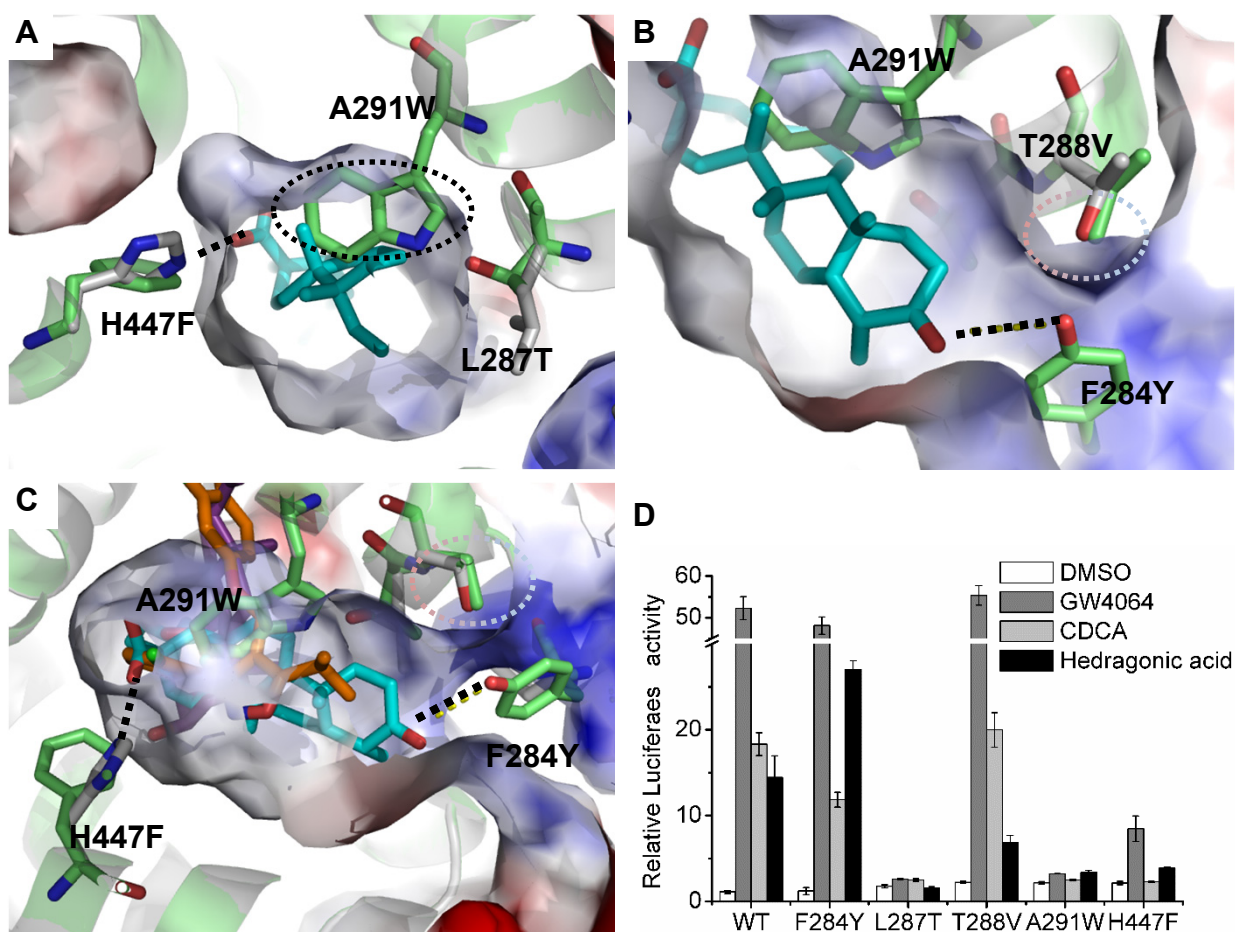


Figure 5

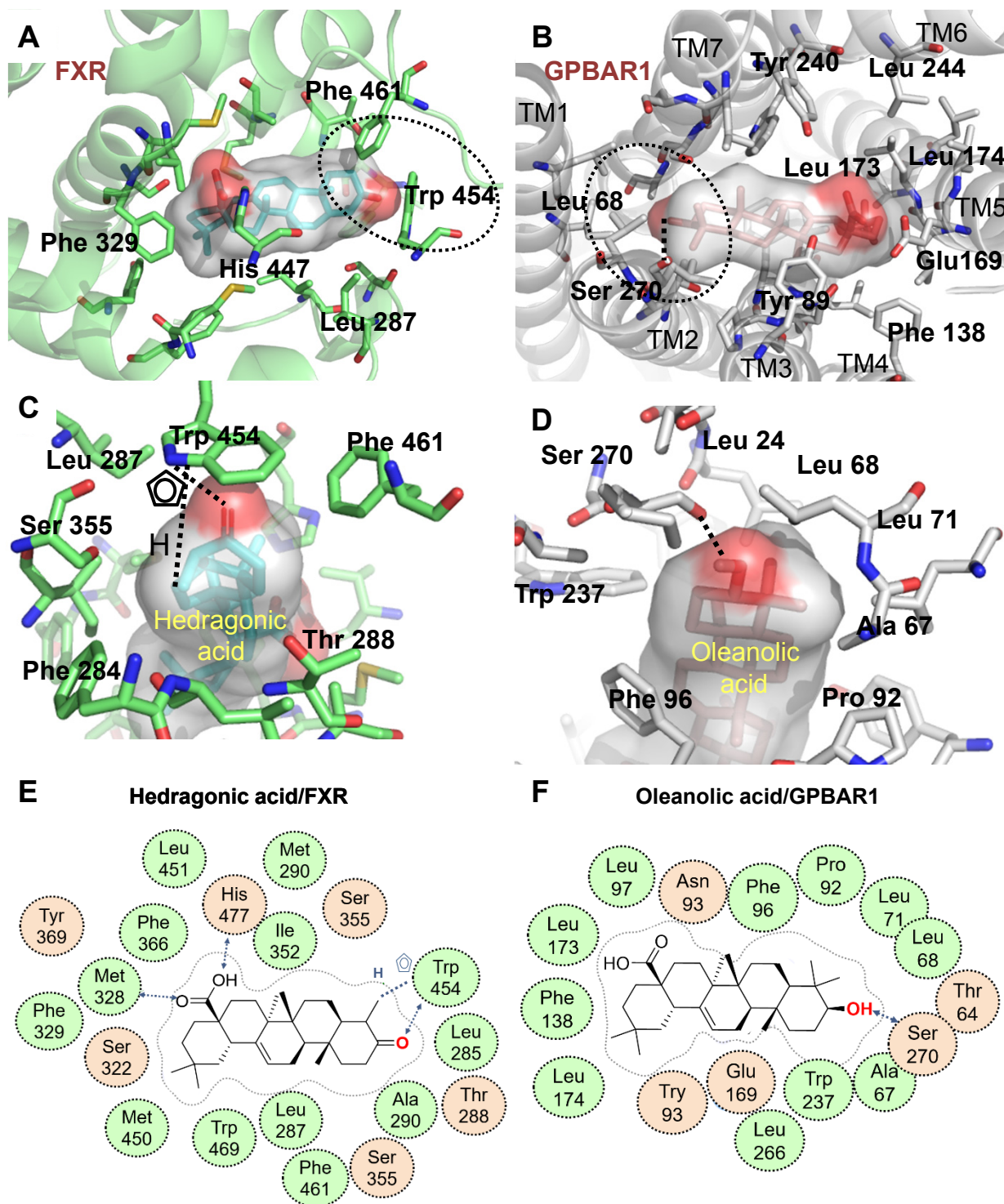
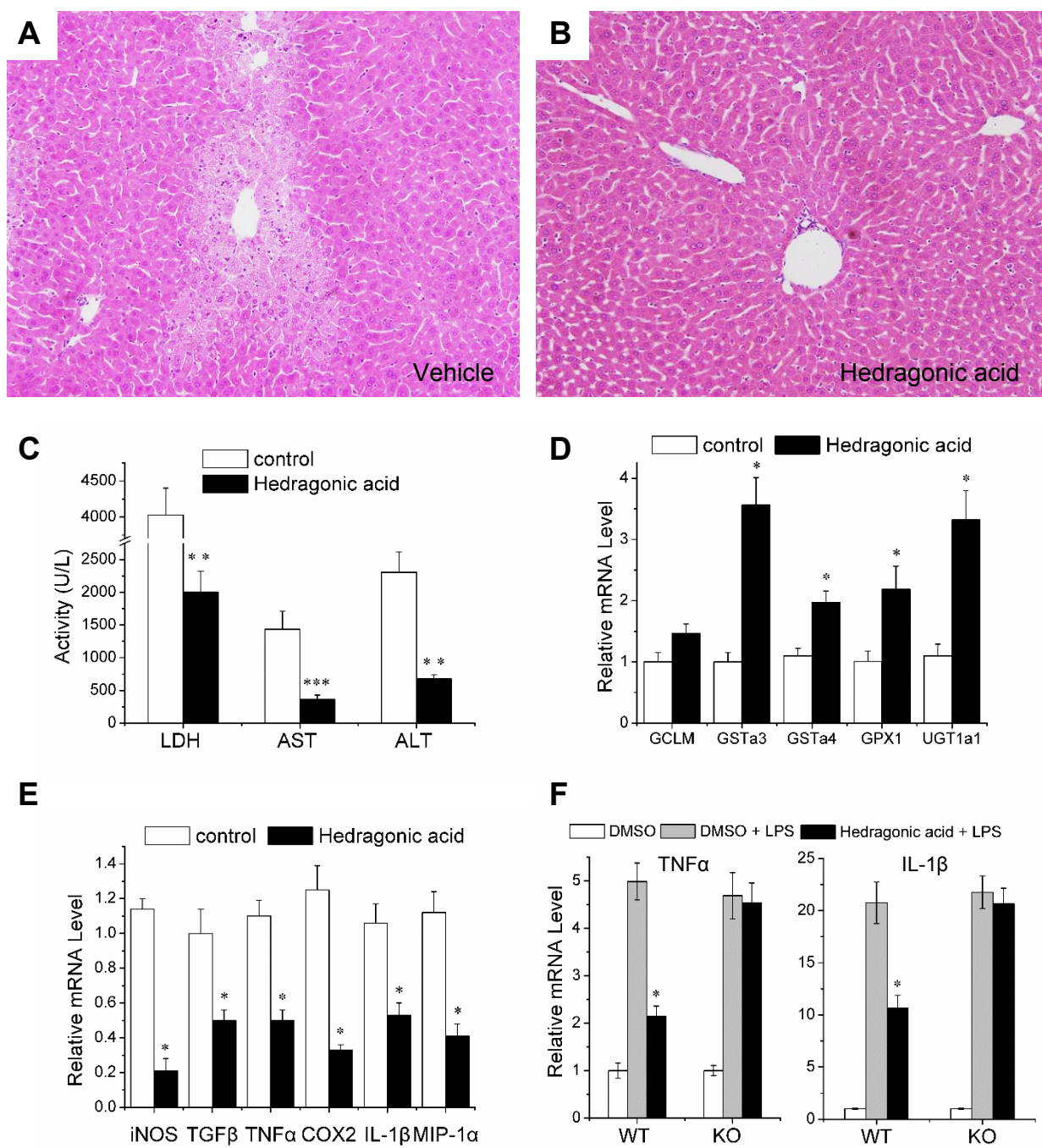


Figure 6



MOLECULAR PHARMACOLOGY

Identification of an Oleanane-type Triterpene Hedragonic Acid as a Novel Farnesoid X Receptor Ligand with Liver Protective Effects and Anti-inflammatory Activity

Yi Lu, Weili Zheng, Shengchen Lin, Fusheng Guo, Yanlin Zhu, Yijuan Wei, Xi Liu, Shikai Jin, Lihua Jin and Yong Li

State Key Laboratory of Cellular Stress Biology, School of Life Sciences, Innovation Center for Cell Signaling Network, Xiamen University, Xiamen, Fujian 361005, China

*Correspondence:

Email: jinh@xmu.edu.cn (L.J.), Tel: +86-592-2181560; yongli@xmu.edu.cn (Y.L.), Tel: +86-592-2181510.

Supporting Information

Supplemental Table 1. The sequences of primers used in RT-PCR.

Supplemental Figure 1. The relative mRNA levels of FXR target genes regulated by compounds in hepatocytes from male mice.

Supplemental Figure 2. The relative mRNA levels of FXR target genes regulated by compounds in hepatocytes from female mice.

Supplemental Figure 3. The molecular structures of FXR or GPBAR1 ligands.

Supplemental Table 2. Data collection and refinement statistics.

Supplemental Figure 4. The different shape prosperities of oleanolic acid and hedragonic acid.

Supplemental Table 3. The calculated molecular shape properties of oleanolic acid and hedragonic acid.

Supplemental Table 5. Structural validation of the docking models of oleanolic acid- and hedragonic acid-bound GPBAR1 by mutagenesis assays.

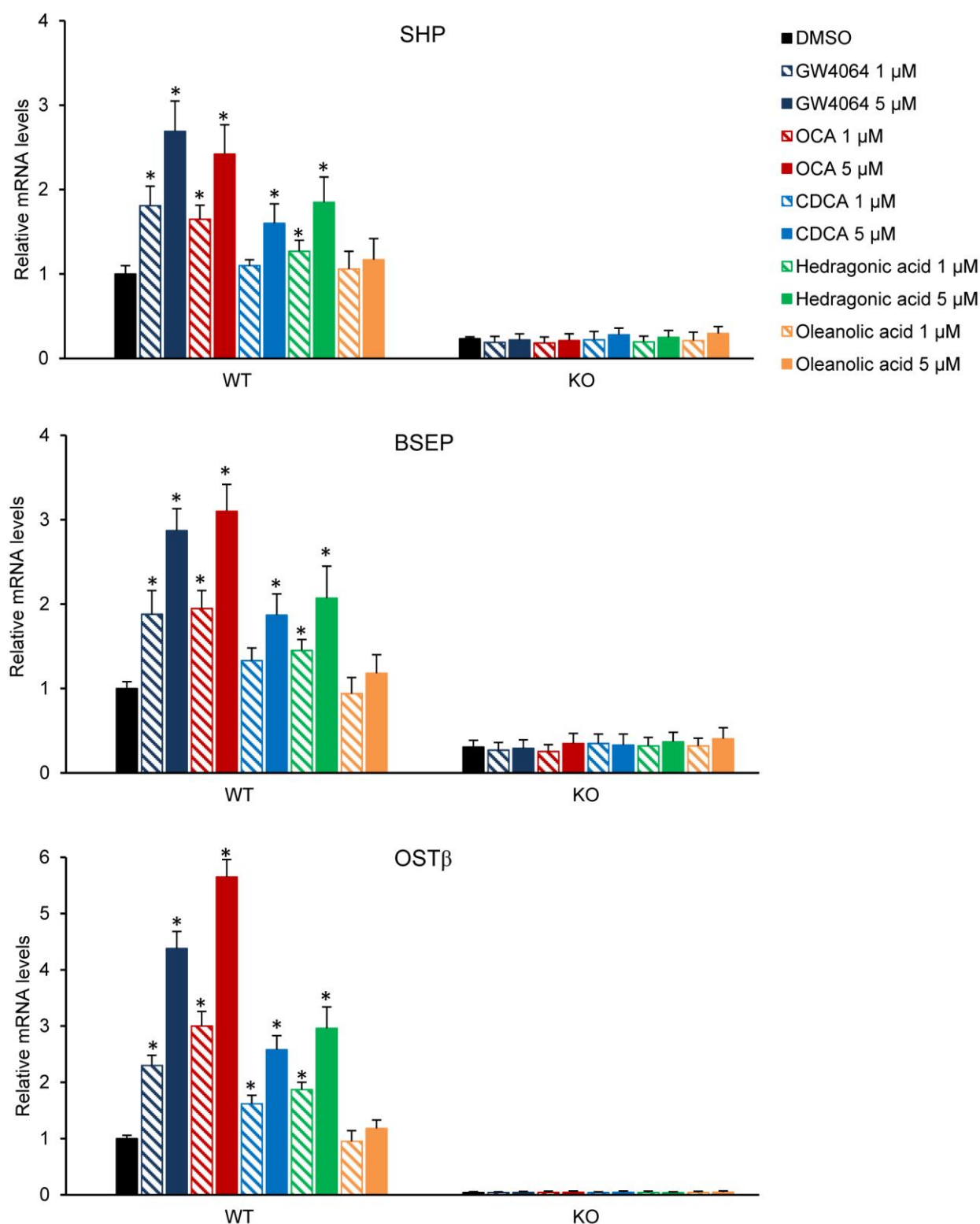
Supplemental Table 1 The sequences of primers used in RT-PCR.

Genes	Primer Sequences	
TGF β	<i>F</i>	CACTGATACGCCTGAGTG
	<i>R</i>	GTGAGCGCTGAATCGAAA
IL-1 β	<i>F</i>	AGAGCATCCAGCTTCAAATC
	<i>R</i>	GCTTCTCCACAGCCACAAT
TNF α	<i>F</i>	GTAGCCACGTCGTAGCAAAC
	<i>R</i>	AGTTGGTTGTCTTTGAGATCCATG
COX2	<i>F</i>	TGAAAGCCCTCTACAGTGAC
	<i>R</i>	GTGCTCCAAGCTCTACCAT
MIP-1 α	<i>F</i>	GCTCCAGCCAGGTGTCATTT
	<i>R</i>	AGGCATTCAAGTCCAGGTCAG
GPX1	<i>F</i>	GTGTGCCGCAACGACATTG
	<i>R</i>	CTATGTCAGGTTGATGTCTG
UGT1a1	<i>F</i>	TCACTGGGAAGTTGTGCAAC
	<i>R</i>	GAGAATACTCAAAGAGACTGTC
GCLM	<i>F</i>	GGCTTCGCCTCCGATTGAAG
	<i>R</i>	TCACACAGCAGGAGGCCAGGT
GST α 3	<i>F</i>	GACTAAGTGTTGACCCTACTTAG
	<i>R</i>	GAATACTCCAGAGTCTAAGAAGC
GST α 4	<i>F</i>	CTGCTGCAGGCATTTAAGAC
	<i>R</i>	TTCTGGAATGCTCTGCAGC
iNOS	<i>F</i>	GGCAGCCTGTGAGACCTTTG
	<i>R</i>	GCATTGGAAGTGAAGCGTTTC
SHP	<i>F</i>	TGGGTCCCAAGGAGTATGC
	<i>R</i>	CAGTGATGTCAACGTCTCC
BSEP	<i>F</i>	GGGAGCAGTGGGTGTGGTAAAAG
	<i>R</i>	TCCTGGGAGACAATCCCAATGTT
OST β	<i>F</i>	GACAAGCATGTTCTCCTGAGA
	<i>R</i>	TGTCTTGTGGCTGCTTCTTTC
GAPDH	<i>F</i>	GCCTCCGTGTTCTACCC
	<i>R</i>	TGCCTGCTTCACCACCTTC

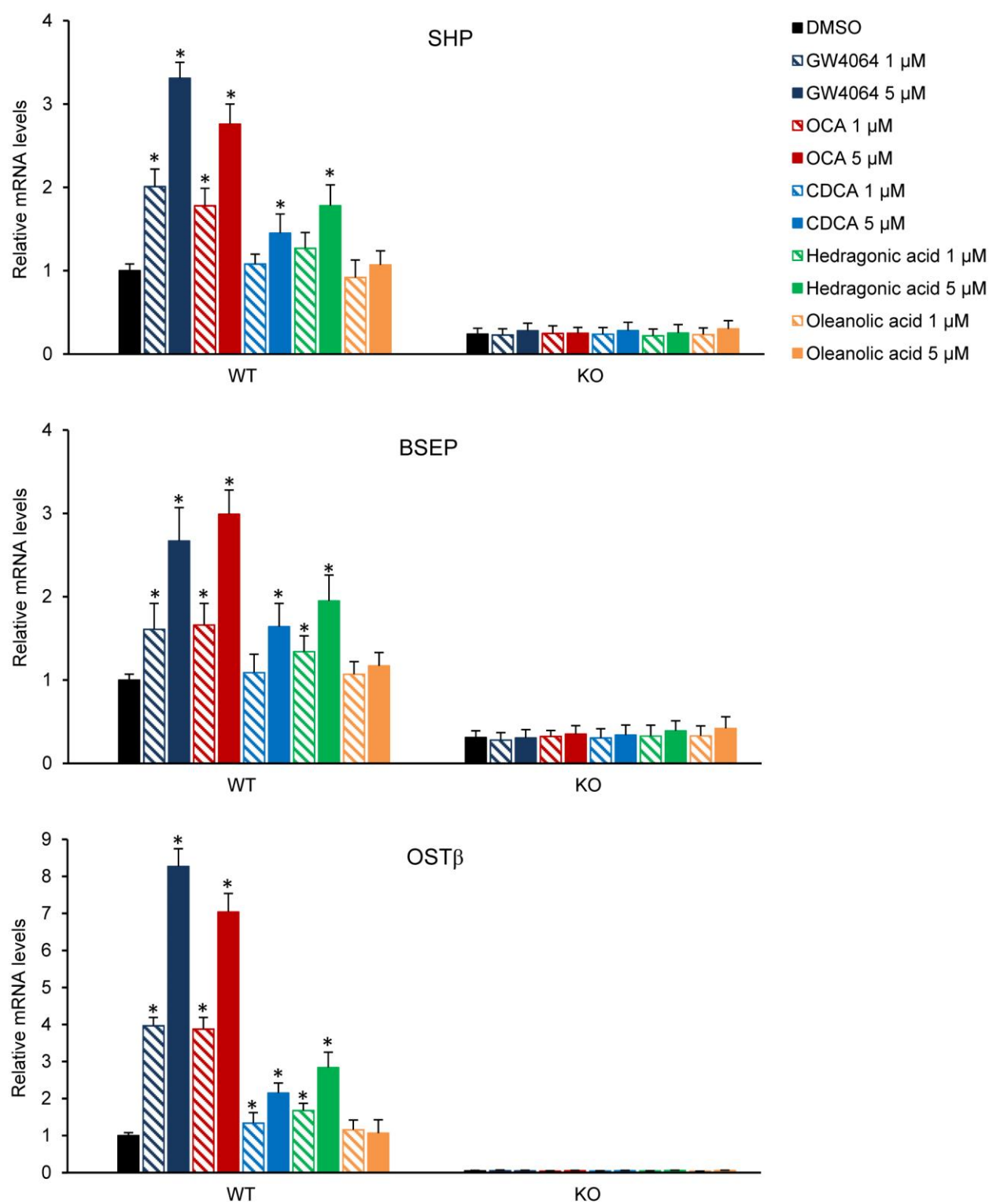
Supplemental Table 2 Data collection and refinement statistics.

Data collection	FXR/Hedragonic acid/SRC2-3		
Space group	C2221		
Cell dimensions			
<i>a</i> , <i>b</i> , <i>c</i> (Å)	74.558	86.073	177.296
<i>a</i> , <i>b</i> , <i>g</i> (°)	90.000	90.000	90.000
Resolution (Å)	50-2.91		
<i>R</i> _{merge}	0.085 (0.586)		
<i>No. of total/unique reflections</i>	26857/12900		
<i>I</i> / <i>σI</i>	30.1(1.52)		
Completeness (%)	88		
Redundancy	7.9(1.2)		
Refinement:			
Resolution (Å)	2.91		
No. reflections	10215		
<i>R</i> _{work} / <i>R</i> _{free}	0.238/0.286		
No. atoms			
Protein	1701		
Ligand/ion	48		
Numbers of Water	18		
<i>B</i> -factors			
Protein	81.401		
Ligand/ion	71.514		
Water	92.558		
R.m.s. deviations			
Bond lengths (Å)	0.0119		
Bond angles (°)	2.2003		
Ramachandran			
favoured	364	86%	
Allowed	55	13%	
outliers	4	1%	

Values in parentheses are for highest-resolution shell.

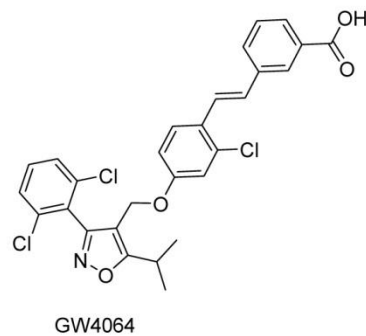
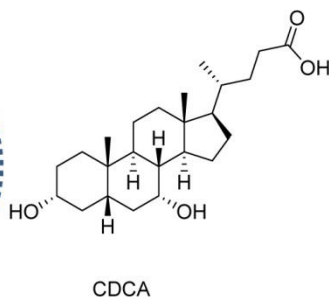
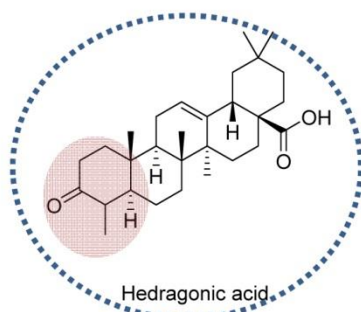


Supplemental Figure 1. The relative mRNA levels of FXR target genes regulated by compounds in hepatocytes from male mice. Primary hepatocytes were isolated from wild-type (WT) and FXR knock-out (KO) male mice. After treated with two doses of GW4064, obeticholic acid (OCA), CDCA, hedragonic acid and oleanolic acid respectively for 24 hours, real-time quantitative PCR were performed to measure the mRNA levels of SHP, BSEP and OSTβ. Relative mRNA levels were normalized to GAPDH levels.

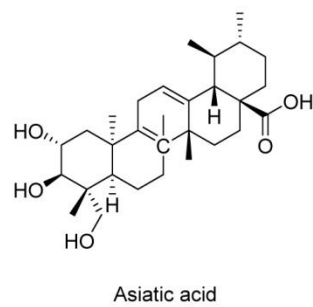
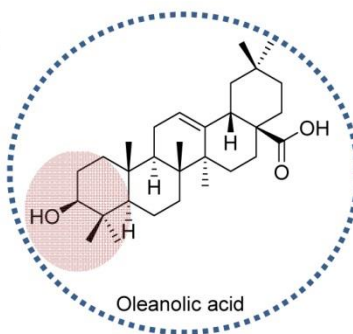
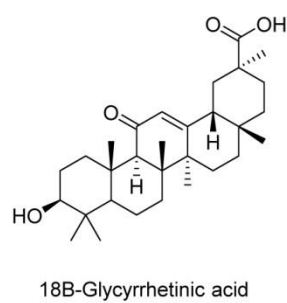
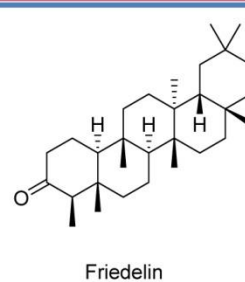
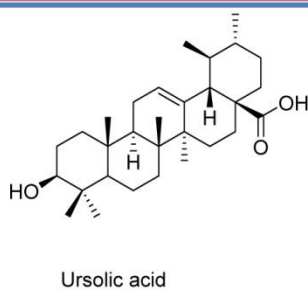
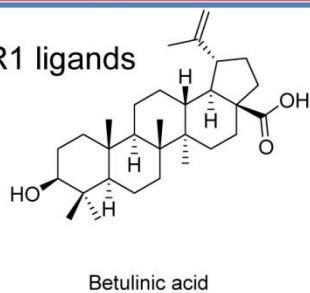


Supplemental Figure 2. The relative mRNA levels of FXR target genes regulated by compounds in hepatocytes from female mice. Primary hepatocytes were isolated from wild-type (WT) and FXR knock-out (KO) female mice. After treated with two doses of GW4064, obeticholic acid (OCA), CDCA, hedragonic acid and oleanolic acid respectively for 24 hours, real-time quantitative PCR were performed to measure the mRNA levels of genes SHP, BSEP and OSTβ. Relative mRNA levels were normalized to GAPDH levels.

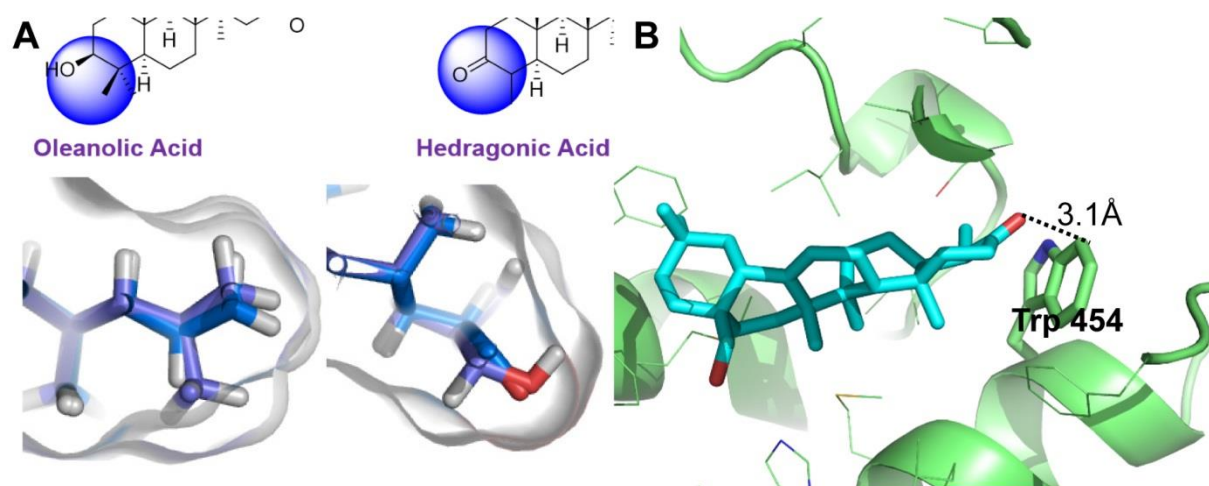
FXR ligands



GPBAR1 ligands



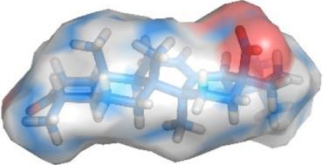
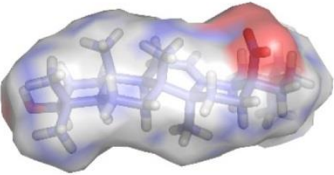
Supplemental Figure 3. The molecular structures of FXR or GPBAR1 ligands.

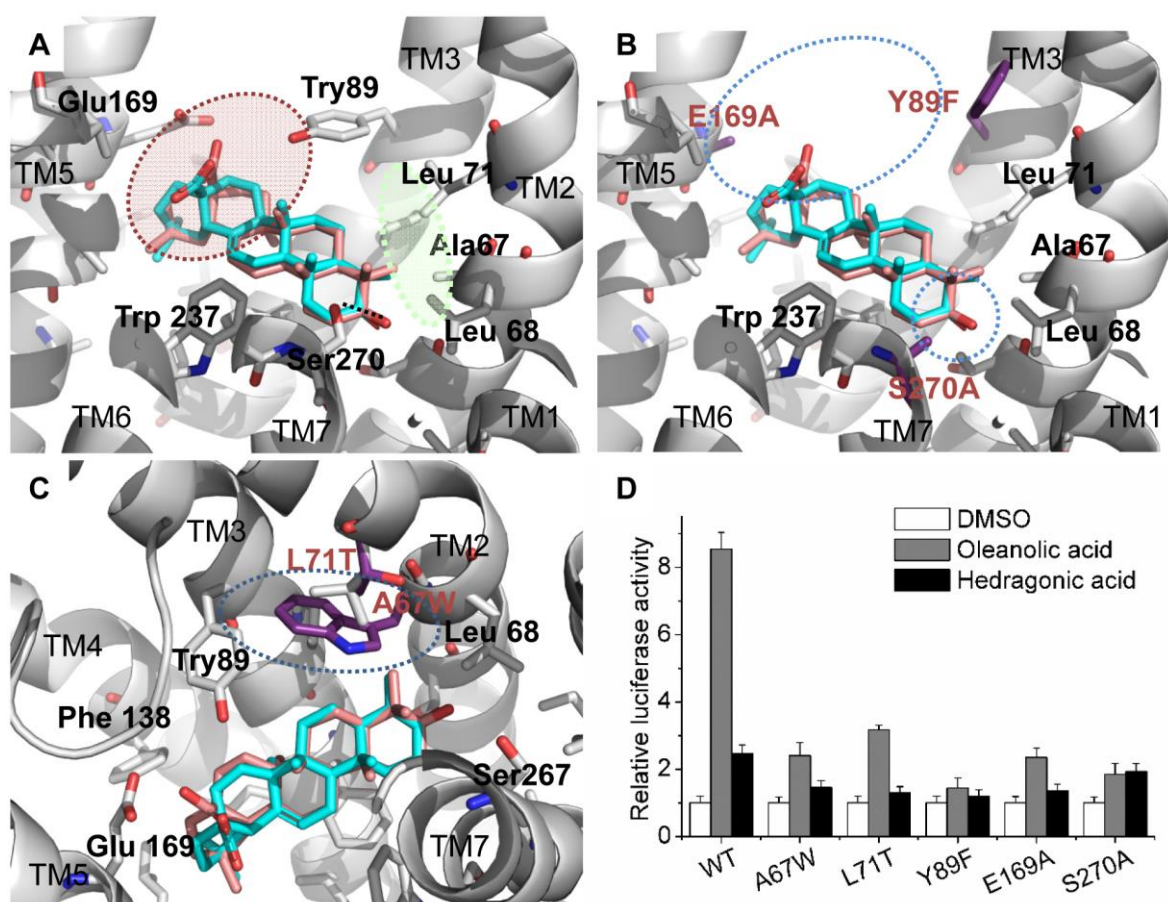


Supplemental Figure 4. The different shape prosperities of oleanolic acid and hedragonic acid.

(A) The alignment of structures of hedragonic acid and oleanolic acid. Structures are shown in stick representation. The carbon atoms are depicted in blue and purple for hedragonic acid and oleanolic acid, respectively; the oxygen atoms are in red. The VWD-surface was created by PYMOL. (B) The structure of hedragonic acid bound with FXR LBD in carton representation. FXR LBD is in light green and the bound hedragonic acid is shown in stick representation with carbon and oxygen atoms depicted in cyan and red, respectively. The distance between the oxygen atom of hedragonic acid and Trp454 of FXR is measured in crystal structure by Coot.

Supplemental Table 3 The calculated molecular shape properties of oleanolic acid and hedragonic acid.

Name of molecules	VDW- area \AA^2	VDW- volume \AA^3	Polar volume \AA^3			
			1 \AA	2 \AA	3 \AA	4 \AA
 Hedragonic acid	461.24	653.44	9	0	0	0
 Oleanolic acid	493.75	685.22	28.5	6.125	2.5	0.5



Supplemental Figure 5. Structural validation of the docking models of oleanolic acid- and hedragonic acid- bound GPBAR1 by mutagenesis assays. (A) The docking mode of oleanolic acid to GPBAR1. GPBAR1 is in grey, the polar interaction environment is marked by dashed red circle, the hydrophobic cavity formed by Leu71, Leu68 and Ala67 is indicated by dashed green circle. The hydrogen bond is indicated with a dashed black line. (B) The mutations Y89F and E169A damaged the polar interaction of ligands in the pocket of GPBAR1. (C) The mutations A67W and L71T destroyed the hydrophobic environment for ligand binding. In (B) and (C), the mutated residues were shown in purple, and the dashed blue circles indicate the abolished interactions when these positions were mutated. (D) Validation of the five crucial interaction sites on GPBAR1 by mutagenesis assays. HEK-293T cells were co-transfected with plasmids encoding full-length GPBAR1 or mutants and pCRE-luc reporter. Hedragonic acid and oleanolic acid were added 5 h after transfection. Cells were harvested 24 h later for the luciferase assays with the Dual-Luciferase Reporter assay system. The luciferase activities were normalized to renilla activity co-transfected as an internal control. Values are the means \pm s.e.m. of three independent experiments.